Journal of Archaeological Science: Reports 41 (2022) 103303

Contents lists available at ScienceDirect

Journal of Archaeological Science: Reports

journal homepage: www.elsevier.com/locate/jasrep

Mineralogical transformations due to salt whitening agent in modern Hebron ceramics

L. Teodorescu [a,b,*], N. Cantin [a], A. Ben Amara [a], R. Chapoulie [a], V. Roux [c]

[a] IRAMAT-CRP2A, UMR 5060, CNRS, University Bordeaux Montaigne, Maison de l'Archéologie, Domaine Universitaire, Esplanade des Antilles, 33607 Pessac Cedex, France

[b] Department of Materials Science and Engineering, University of Pitesti, Romania

[c] Préhistoire et Technologie, UMR 7055, CNRS, University of Paris Nanterre, 21 Allée de l'Université, 92023 Nanterre Cedex, France

ARTICLE INFO

Keywords:
Ceramic
Hebron
Salt NaCl
Whitening
Firing process
Colorimetry
Petrography
XRD
SEM-EDX

ABSTRACT

The aim of this research is to investigate the influence of NaCl on the colours and chemical composition of Ca-rich ceramic bodies. The addition of salt to ceramics is a practice that has been observed in several potter communities where the addition of salt is explicitly intended to whiten ceramics. In order to conduct this research and characterize the physico-chemical properties induced by the presence of salt, raw clay material and pot sherds were collected from the modern production at Hebron. Experimental bricks were made using two clayed sediments: one with a low CaO content (<10%) and one with a higher CaO content (20–25%). Different proportions of NaCl were added (up to 5%) to clay pastes which were fired at different temperatures. Mineralogy (petrography, XRD), chemistry (SEM-EDX) and colour analyses were carried out on raw clay materials, pot sherds and experimental (lab-made) bricks. SEM imagery offered the possibility to monitor the evolution of the mineralogical transformations, the pore system with increasing firing temperature and salt content. Results confirm the role of salt as a catalyst in the transformation reaction of calcium silicates during the firing process and its influence on the colour of the finished object.

1. Introduction

Salt has long been used by potters in various forms because they knew the different effects produced on their ceramics, especially a whitening effect (Brooks et al., 1974). Indeed, the use of salt to obtain white pottery, in the form of salted clay (salted water or added salt), is noted in Mesopotamia and can still currently be found in a diversity of countries, from Central America to the Indian subcontinent (Rye, 1976; von der Crone and Maggetti, 1998). The question of the physico-chemical properties induced by the presence of salt continue to intrigue, as several scientific studies have been conducted to better understand the effect of halite in ceramic production, from an analytical point of view. For example, Rye (1976) highlighted conspicuous cubic voids in thin sections, which were interpreted as pseudomorphs of salt crystals.

The effects produced during firing by the presence of sodium chloride in a Ca-rich ceramic body (obtained from a carbonate-rich clayey material) are numerous and wide-ranging (Bearat et al., 1989; Combès and Louis, 1967). In various studies, it has been pointed out that the use of salt in addition to raw clay material prevents the hydration of the CaO grains after firing (Rye, 1976). The presence of chlorides, such NaCl, also accelerates and participates in the dissociation reaction of calcite. The resultant decarbonation of the $CaCO_3$ increases the porosity of the paste (Bearat, 1990). Furthermore, salt can be considered as a discoloration agent in ceramic pastes produced from these carbonate-rich clays (Dufournier, 1982). Finally, the use of salt can also cause a partial disappearance of potassium in Ca-rich pastes during firing (Fabbri & Fiori, 1985). According to previous works, it was observed that the maximum addition of salt to the clay material was 5% (Rye, 1976). As for the firing temperature range, Fabbri and Fiori (1985) noticed that with 2% of salt addition, crystalline phases such as gehlenite and diopside start to appear at 700 °C. In addition, Bearat (Bearat et al., 1989) specified that the alkalin chlorures will typically start to volatize with the addition of NaCl at temperatures of 700–750 °C.

The aim of this research was to develop a multi-approach methodology in order to better understand the effects of salt NaCl in terms of

* Corresponding author at: IRAMAT-CRP2A, UMR 5060, CNRS, University Bordeaux Montaigne, Maison de l'Archéologie, Domaine Universitaire, Esplanade des Antilles, 33607 Pessac Cedex, France.

E-mail address: laura.teodorescu93@gmail.com (L. Teodorescu).

https://doi.org/10.1016/j.jasrep.2021.103303
Received 31 May 2021; Received in revised form 10 November 2021; Accepted 29 November 2021
Available online 17 December 2021

whitening and the physico-chemical changes which occur in the ceramic body. Furthermore, elaborated experimental bricks were manufactured by varying the salt content and the firing temperatures, with the same raw materials as those used by the Hebron potters for their production.

2. Materials and methods

2.1. Ethnographic context

An ethnographic survey was recently conducted in Hebron (Palestinian territories) by V. Roux. In her study, she found that potters used four different types of raw materials for producing utilitarian vessels: yellow clay sediment (noted as YC), red clay sediment (terra rossa) (noted as RC), sand and salt (Fig. 1). The volumic proportion between YC and RC is 2:1. Meanwhile, sand accounts for 1/6 of the total paste volume. The red clay sediment is said to give its yellow counterpart more plasticity. This serves to prevent rapid shrinkage when drying, and to avoid accidents during the firing process (bloating). The yellow clay material is brought from construction sites located in the region of Hebron. The YC is most likely from the Moza Formation (upper Cenomanian stage). The Moza Formation extends throughout the southern central hills of the southern Levant, from north of Jerusalem to south of Hebron. On the other hand, the red clay is acquired from neighboring lands and is a type of agricultural soil. The terra rossa (RC) can come from any place, but more probably on the more leached soil (without carbonates) that develops on hard limestone and dolomite.

The sand is collected from local mountains and added to the clay. Since the early 1970's, fires used in ceramic production have largely been fueled with tires, resulting in firing temperatures rapidly rising to approximately 1000 °C. Subsequently, thermal shock and breakage while firing is a critical consideration. The addition of sand thus helps prevent cracking of the vessel while it is being fired. The sand is added to the yellow and red clay material in a mixing tank. The salt, taken from local shops, is then added during the wedging process (Fig. 1 right).

It is said by potters that the salt is added for the pots to become white and for the clay to "better behave". Overall, the clay preparation includes the following main steps: a) drying the clay materials; b) mixing the yellow and red clay material with the sand in water mixing tanks; c) pouring the liquid clay material in a soaking tank through a nylon screen; d) following the complete wetting of the clay material, one then pours the liquid material in a drying tank; and e) after the solidification of the clay, it is wedged with a pug mill. During this final stage, the salt is added in amounts up to 0.5% of the quantity of clay paste to be wedged according to the potters.

2.2. Materials

In this study, the sampling consists in four modern potsherds and four raw materials (which are used by the Hebron potters in their manufacture), collected in Hebron. The modern sherds were selected by visual aspects, representing two types of ceramic bodies: a white and a pink ceramic sherd. The raw clay materials included both yellow (YC) and red (RC) clayey sediments, the sand temper, and the salt used for achieving a whitening effect.

Fig. 1. Raw materials: yellow clay, red clay, and sand (left image). Wedging the clay with a pug mill. It is at this stage that the salt is added to the clay paste (right image). (photographs by V. Roux). (For interpretation of the references to color in this figure legend, the reader is referred to the web version of this article).

In addition, for enlarging our understanding of the whitening effect and the parameters involved in the mechanism of the firing process on Hebron ceramic, 18 experimental bricks have been manufactured in the laboratory of IRAMAT-CRP2A (Bordeaux), using the same clays used by the Hebron potters (Table 1). The preparation of the briquettes consisted in using 20 g of each clay sediment (previously desegregated), to which salt was added in different proportions: 0%, 2% and 5% of total clay by weight. Due to the absorption effect, the red sediment was mixed with 10 ml of water, and the yellow sediment, with 15 ml. After, they were placed on an aluminum container and allowed to air-dry at room temperature for 48 h. The experimental bricks were fired in an electric kiln at 750 °C, 900 °C and 1000 °C, in an oxidizing atmosphere. The temperature was raised at a heating rate of 100 °C/h, with a soaking time of three hours and cooling down to room temperature (Fig. 2).

2.3. Methods

The methodological protocol encompasses a multitude of analytical techniques (petrographic, cathodoluminescence, SEM-EDX, XRD, colorimetry) to ensure representativeness and complementarity of observations.

Before analyzing the potsherds and the experimental bricks, the grain size distribution of the raw materials was first performed using a Laser Diffraction particle size analyser Horiba LA-950 device in order to characterize their properties and evaluate clay plasticity. The raw material - samples were treated with oxygenated water (H_2O_2) and sodium hexametaphosphate ($Na_6O_{18}P_6$). They were diluted before pipetting to 300 ml, and placed in the grain size sampler. Grain sizes were then reported as broader classes according to Konert and Vandenberghe (1997) classification system: clays [<7 μm], silts [7–63 μm], and sands [63 μm–2 mm]. Color of the material studied were monitored using a Konica Minolta CM-2600D portable spectrophotometer (360–740 nm) with a spectral resolution of 10 nm and a diameter area of 8 mm. The standard illuminator was D65 using CIE 1964 10° standard observer. The calibration was performed with a black and white reference set to SCI (spectral reflection included) mode. Cathodoluminescence (CL) was then utilized mainly to follow the evolution of mineralogical phase changes in the experimental bricks. The device employed was a Cathodyne Microvision instrument coupled with a Leica M125 binocular lens and a Leica DFC4500 digital camera to capture images with the LAS software. The electron gun was fixed and positioned at 45° to the surface

Table 1
Procedure for the preparation of the 18 experimental bricks.

Salt NaCl	Clay type	Firing Temperature (°C)	Sample ID Name
0 %	YC	750	YC 0% 750 °C
		900	YC 0% 900 °C
		1000	YC 0% 1000 °C
	RC	750	RC 0% 750 °C
		900	RC 0% 900 °C
		1000	RC 0% 1000 °C
2 %	YC	750	YC 2% 750 °C
		900	YC 2% 900 °C
		1000	YC 2% 1000 °C
	RC	750	RC 2% 750 °C
		900	RC 2% 900 °C
		1000	RC 2% 1000 °C
5 %	YC	750	YC 5% 750 °C
		900	YC 5% 900 °C
		1000	YC 5% 1000 °C
	RC	750	RC 5% 750 °C
		900	RC 5% 900 °C
		1000	RC 5% 1000 °C

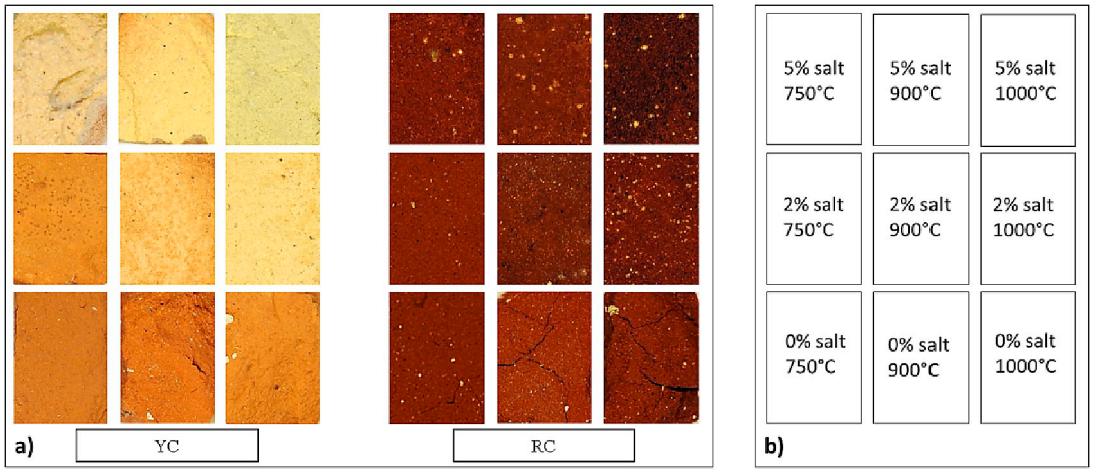

Fig. 2. (a) Colour surface of experimental samples made from yellow (YC) and red clay (RC) sediments; (b) the protocol used per sample (salt content and firing temperature). (For interpretation of the references to color in this figure legend, the reader is referred to the web version of this article.)

of the sample. The exposure time for the CL images was 15 s with a current intensity of 10 μA. Petrography allowed for the characterisation of the minerals and rocks present in the ceramic body, where identifiable. For this, a Leica DM2500 polarizing microscope was used with objectives from 2.5 to 40.

The XRD powder measurements were performed to identify the mineral constituents of both raw materials and experimental bricks, and for the orientation of deposits to discriminate the clay mineral species. This was completed using a Bruker diffractometer (D8-Advance, set in Bragg-Brentano reflection mode) a X-ray tube with Cu Kα radiations operating at 40 kV and 40 mA. The measurements were recorded from 3° to 60°, with a scan step size of 0.01° and an acquisition time/step of 1 s. Qualitative analysis of the obtained diffractograms was realized with the EVA software using the PDF − 2008 database from ICDD. In addition, a Rietveld refinement was applied by using TOPAS software, to quantify the mineral phases. For analyzing clay minerals on oriented slides, it was first necessary to eliminate the carbonates without attacking the clay phases. For this, a weak acid solution with a buffer at pH 5 was used. The oriented slides were then submitted to ethylene glycol and heat treatments (at 350 °C and 550 °C) according to Bouchet et al. (2000).

SEM imagery (JEOL – IT500 HR) facilitated the observations of the micro-texture of the modern potsherds and briquettes in thick sections, as well as the progress of the mineral transformations upon firing. The microscope was used in Low Vacuum mode with a pressure of 30 Pa. The parameters used for the analysis of the samples included the acceleration voltage of 20 kV, with the probe current from 10^{-10} to 5.10^{-9} A and about 4 000 000 counts per second. The acquisition of the spectra (performed with a double EDX, Oxford Instruments UltimMax 100) was done on the thick polished sections of the ceramic bodies and on pressed pellets. Finally, the analyse was performed using Oxford Instruments AZtec NanoAnalysis. The standard corrections were calculated using the software's internal standard. The quantification of chemical composition was obtained from the average of 4 areas of 0.58 mm^2 each. All results were expressed in wt% oxides (normalized to 100%), thus making it possible to quantify the major and minor elements (Na_2O, MgO, Al_2O_3, SiO_2, SO_3, K_2O, CaO, TiO_2 and Fe_2O_3), while Cl was expressed in simple wt.

3. Results and discussion

3.1. Mineralogical and chemical characterisation of raw materials

Results concerning grain size distribution revealed that the yellow clay sediment (YC) has a higher concentration of particles smaller than 7 μm compared to the red clay sediment (RC) (Table 2). Furthermore, approximately 26% of the particles in the red clay sediment are larger than 16 μm and are distributed between coarse silt (17%) and fine sand (9%). In contrast, the yellow clay sediment is mainly composed of particles smaller than 16 μm, ranging from fine silt (37%) to clay particles (58%). The sand used as temper consists of 75% fine sand and 16% coarse sand. Regarding the salt, it contains approximately 79% coarse particles, with sizes between 16 and 500 μm.

X-ray diffraction analysis showed that the two clay sediments used by the Hebron potters have a similar mineralogical composition, composed of clay minerals, calcite, quartz, iron oxides (for RC) and iron hydroxides (for YC), potassium feldspars and plagioclases. However, YC is richer in potassium feldspar and calcite. Finally, the analysis of the oriented slides allows the precise identification of the clay minerals detected during the powder analysis. The yellow clay sediment consists of a large quantity of kaolinite, a smaller proportion of a mixed layer clay around 11.3 Å (Illite/Vermiculite), illite and a small proportion of chlorite. The RC sediment has a similar clay mineral composition but the proportions differ. The proportion of kaolinite is lower in this sediment and the ratio of the others minerals (I/V, Ch, I) are therefore higher, giving this raw clay material more plasticity.

The chemical analysis by SEM-EDX indicates that the both clayey sediments are rich in calcium (Table 3), the yellow sediment being more calcium-rich with 23% CaO. The potassium content is also higher (3.5% K_2O), which may be related to the presence of the orthoclases detected

Table 2
Grain size distribution of raw materials of Hebron.

Sample	% coarse sand (500–2000 μm)	% fine sand (63–500 μm)	% coarse silt (16–63 μm)	% fine silt (7–16 μm)	Clay (<7 μm)
Red Clay Sediment (RC)	0	9	17	27	46
Yellow Clay Sediment (YC)	0	1	4	37	58
Salt	0	41	28	21	11
Sand temper	16	75	2	3	4

Table 3
Chemical composition (wt%), obtained by SEM-EDX (powders pellets for raw materials and thick sections for sherds and experimental samples (SD – standard deviation, dl – detection limit).

		Na_2O	MgO	Al_2O_3	SiO_2	SO_3	Cl	K_2O	CaO	TiO_2	Fe_2O_3	K_2O/SiO_2
Raw Materials	Sand	0.1	0.2	1.9	95.0	0.2	<dl	<dl	1.2	0.5	0.9	
	SD	0.1	0.1	0.1	0.3	0.1			0.1	0.1	0.1	
	Salt	46.2	0.1	0.2	0.7	1.8	49.2	0.2	1.6	<dl	0.2	
	SD	0.1	0.1	0.1	0.1	0.2	0.1	0.1	0.1		0.1	
	YC	0.2	2.3	18.7	42.6	0.2	<dl	3.5	23.3	0.8	8.3	
	SD	0.1	0.1	0.3	0.7	0.1		0.1	0.5	0.1	0.7	
	RC	0.4	2.2	18.5	57.3	0.1	<dl	1.5	8.9	1.4	9.8	
	SD	0.1	0.1	0.1	0.1	0.1		0.1	0.2	0.1	0.1	
Modern sherds	White sherd 1	2.3	2.9	14.4	45.5	1.9	1.6	3.0	22.2	0.7	5.6	0.066
	SD	0.1	0.1	0.2	0.5	0.1	0.1	0.1	0.2	0.1	0.1	
	White sherd 2	2.1	2.8	13.7	47.0	1.8	1.4	2.9	21.9	0.8	5.6	0.062
	SD	0.1	0.1	0.5	1.4	0.1	0.1	0.2	0.4	0.1	0.1	
	Pink sherd 1	0.9	3.4	14.1	50.1	0.7	0.2	2.5	20.4	0.8	6.7	0.050
	SD	0.1	0.1	0.2	0.5	0.1	0.1	0.1	0.2	0.1	0.2	
	Pink sherds 2	0.8	3.4	14.0	51.2	0.8	0.2	2.5	19.8	0.9	6.4	0.049
	SD	0.1	0.1	0.4	0.9	0.1	0.1	0.1	0.2	0.1	0.3	
Experimental bricks	YC 0% 750 °C	0.2	2.9	20.2	49.1	<dl	0.5	3.8	16.7	0.9	5.8	0.077
	SD	0.1	0.1	0.3	0.4		0.1	0.1	0.4	0.1	0.2	
	YC 2% 750 °C	1.3	2.9	18.0	45.0	0.1	1.2	3.5	21.3	0.8	5.7	0.078
	SD	0.4	0.2	0.3	0.6	0.1	0.1	0.2	0.4	0.1	0.2	
	YC 5% 750 °C	3.1	2.9	17.6	44.1	0.2	2.2	2.0	21.8	0.8	5.1	0.045
	SD	0.5	0.1	0.4	0.7	0.1	0.1	0.2	0.8	0.1	0.1	
	YC 0% 900 °C	0.1	3.0	18.9	44.7	0.1	0.3	3.7	22.4	0.8	5.9	0.083
	SD	0.1	0.1	0.3	0.2	0.1	0.1	0.1	0.5	0.1	0.1	
	YC 2% 900 °C	1.4	3.1	17.9	45.3	<dl	0.4	2.8	22.6	0.8	5.6	0.062
	SD	0.5	0.1	0.2	0.8		0.1	0.1	0.5	0.1	0.3	
	YC 5% 900 °C	2.0	3.2	17.9	45.2	0.1	0.7	2.0	22.4	0.8	5.5	0.044
	SD	0.5	0.1	0.2	0.3	0.1	0.0	0.5	0.4	0.0	0.3	
	YC 0% 1000 °C	0.1	3.3	18.7	47.0	<dl	0.1	3.4	21.3	0.8	5.1	0.072
	SD	0.1	0.1	0.1	0.2		0.1	0.1	0.3	0.1	0.1	
	YC 2% 1000 °C	1.4	3.5	18.0	46.1	<dl	0.2	1.7	22.8	0.8	5.4	0.037
	SD	0.6	0.2	0.3	1.4		0.1	0.2	0.8	0.1	0.3	
	YC 5% 1000 °C	2.8	3.3	18.4	47.3	0.1	0.2	0.8	21.1	0.8	5.1	0.017
	SD	0.5	0.1	0.3	0.6	0.1	0.1	0.2	0.8	0.1	0.2	

by X-Ray diffraction. Iron and magnesium contents are relatively similar between the two clayey sediments. Therefore, the colour difference between the two clays it is not related to differences in iron content, but rather to its crystallographic form: hematite for the red clay sediment and goethite for the yellow clay sediment according to XRD results. The salt has a high Cl and Na_2O content, which is specific for halite (Table 3). The sand used consists mainly of silica (95%), containing a small proportion of clay minerals, detected by XRD, as impurities.

3.2. Mineralogical and chemical characterisation of modern potsherds

The initial data regarding the microstructure of the modern sherds were obtained by petrographic analysis. The white sherds revealed a significant proportion of inclusions (an estimated 30% by volume) and high quartz content, in which grain diameter ranges from 200 μm and 550 μm. The presence of iron oxides was also noted, as well as a few lithic fragments (quartz-feldspar) and titan oxides. The distribution of inclusions is quite homogeneous and rounded, belonging mainly to the fine sand class. The matrix also presents a dark brown colour with no birefringence. On the other hand, the pink sherds feature a greater density of inclusions (40–50% by volume), among them quartz, iron oxides and biotite are the most notable. Nonetheless, a large amount of similarities in the mineral composition between the pink sherds and white sherds can be confirmed through this petrographic analysis. These similarities include the rounded shape of the inclusions and the presence of specific minerals such as quartz and a few feldspars. Although the samples are mineralogically quite similar, the porosity does differ. In this regard, the pink sherds feature more pronounced and abundant pores as compared to the white sherds.

On the X-Ray patterns, the presence of potassium feldspars, augite or clinopyroxene, gehlenite, and hematite were noticed in both samples. Nevertheless, the peak of halite has been detected only in the white

Table 4
Quantification of mineralogical phases of sherds and experimental samples from Hebron by XRD (Rietveld method).

		illite	quartz	K Feld	Pl Feld	calcite	halite	gehlenite	augite	wollastonite	hematite	spinel	anatase
Modern sherds	White sherd 1	<dl	23,7	0.2	14.9	<dl	0.7	18.2	31.8	9.1	<dl	1.5	1.1
	Pink sherd 1	<dl	30.7	4.3	23.1	<dl	<dl	14.3	20.4	6.1	<dl	<dl	<dl
Experimental bricks	YC 0% 750 °C	26,6	14.5	23.0	<dl	31.3	<dl	<dl	<dl	<dl	1.9	<dl	1.6
	YC 2% 750 °C	18,7	23.0	39.1	<dl	11.7	<dl	<dl	<dl	<dl	5.5	0.1	0.9
	YC 5% 750 °C	<dl	5.9	8.1	12.8	<dl	<dl	19.7	38.5	12.9	0.2	1.6	0.3
	YC 0% 900 °C	<dl	8.1	11.7	19.7	<dl	<dl	29.5	10.1	10.0	4.2	5.7	<dl
	YC 2% 900 °C	<dl	7.3	6.9	22.4	<dl	<dl	23.7	27.4	10.4	0.4	1.1	0.3
	YC 5% 900 °C	<dl	7.1	4.6	18.9	<dl	<dl	22.9	31.1	12.7	0.3	2.3	<dl
	YC 0% 1000 °C	<dl	6.2	12.4	20.2	<dl	<dl	23.1	19.6	14.9	4.5	1.1	<dl
	YC 2% 1000 °C	<dl	6.3	7.1	22.8	<dl	<dl	19.4	27.7	13.7	0.5	2.4	<dl
	YC 5% 1000 °C	<dl	5.7	3.6	20.8	<dl	<dl	14.2	38.6	14.1	<dl	2.5	0.3

sherd (Table 4). Furthermore, it was noticed that the presence of the amorphous phase is more developed in the white sherd than in its pink counterpart. The proportion of Ca-silicates, formed at high temperature (gehlenite, wollastonite) (Cultrone et al., 2001) is also more significant in the white sherd than in the pink one.

Combined, these observations suggest that the sherds were fired under the same conditions (i.e. temperatures), but are yet different due to other factors. For example, the presence of halite is detected in the white sherds and in them Ca-silicates are also higher than in the pink sherds. In addition, a more developed glassy phase and a higher porosity was also noted. These results suggest that more salt had been added to the clay paste of the white sherds than had been added to the pink sherds.

Finally, the bulk chemical composition of the modern ceramic sherds (pink and white), (Table 3) revealed that they have similar chemical composition with high Ca content (20 to 22% CaO) and equivalent percentage of iron (around 6% Fe_2O_3). The two types differ in that the presence of sodium and chlorine, which is more abundant in the white sherds than in the pink sherds.

3.3. Experimental bricks

3.3.1. Colorimetry

The test on the experimental bricks revealed colour changes that are a result of the differences in preparation protocol as described above (see section 2.2). The whitening effect occurred only in the calcium-rich bricks (CaO ~ 23%), prepared with yellow clay (YC). The discoloration effect was initiated by the addition of NaCl. Naked eye observations showed that the fired experimental bricks produced from the red clay sediments are universally red in colour and show little variability in this regard. In contrast, the bricks containing yellow clay sediments without added NaCl have a rather orange colour for all firing temperatures and become more yellow as the NaCl content increases (Fig. 2). In order to describe these colour changes in an objective way, it was necessary to carry out colorimetric measurements. Yet this is only necessary for the bricks produced from yellow clay sediments. As the objective of the study is to focus on the whitening effect of salt, which does not appear to effect the coloration of the red clay sediment containing little amount of calcium (9% CaO), colorimetric measurements for these samples are unnecessary.

When fired at the same temperature, an increase of salt content is associated with a decrease in dominant wavelength. The chromatic coordinates for the sample made with yellow clay, with no salt added and fired at 750 °C, are × = 0.41 and y = 0.37 (Table 5). This colour is situated in the yellow – orange (585–590 nm) range, where the associated dominant wavelength is equal to 586.4 nm (Kelly and Judd, 1976). This colour is non-saturated with the excitation purity (Pe) of 38.7%, highlighting a relatively dark colour with a Y-clarity of 25.4. By contrast, when a yellow clay is fired at 750 °C with 2% NaCl added, the chromatic coordinates are × = 0.40 and y = 0.36. This colour is situated in the orange range (585–600 nm), with the associated dominant wavelength λD = 585.6 nm. A similar increase can be seen when even more NaCl is added. When the yellow clay sample is fired at 750 °C, and 5% NaCl has been added, the λD = 577.0 nm, a value falling within the yellow range (575–580 nm). Simultaneously, a decreasing of excitation purity was noted, indicating a diminution in colour saturation.

Thus, the addition of salt results in the bleaching of the ceramics, as samples to which salt has been added tend to approach the yellow colour (losing the red component). The same observations were made for the other samples produced with yellow clays when fired at 900 °C and 1000 °C. According to the table, the values of clarity (Y as well as L*) increase universally as temperature increases with the highest values corresponding to the addition of 5% NaCl. Overall, the red component (a* positive) decreases in correlation to higher temperature as well as with the increased addition of salt. The lowest value (2.2) corresponds to the YC sample fired at 1000 °C within which 5% NaCl has been added. On the other hand, the yellow component (b* positive) is variable (between 17 and 24) and does not correlate with the variation in firing temperature or the addition of salt. In sum, these results quantify the whitening effect beyond visual descriptions corresponding with measurements reflective of increases in clarity as well as the suppression of the red component (Fig. 3a, b).

Calculating the colour deviation (ΔE*) and comparing to YC 0% samples makes it possible to observe that the colour values rise with the

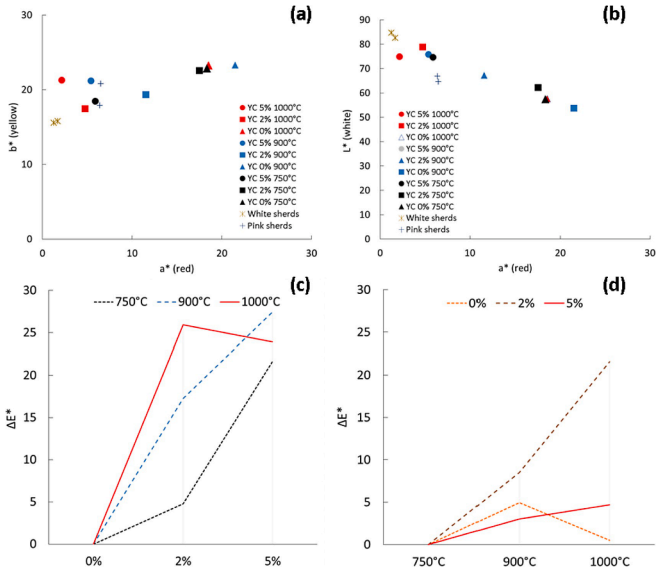

Fig. 3. Chromatic coordinates L*a*b* systems on experimental bricks.

Table 5
Chromatic coordinates of experimental samples, in the (Yxy) and (L*a*b*) systems, with the associated dominant wavelengths λD and P_e (excitation purity).

		λ_D (nm)	Pe (%)	Y	x	y	L*	a*	b*
Modern sherds	White sherd 1	572.7	17.6	65.5	0.346	0.362	84.7	1.3	15.6
	White sherd 2	573.1	18.3	61.3	0.348	0.362	82.5	1.7	15.8
	Pink sherd 1	577.7	25.6	36.4	0.368	0.368	66.8	6.4	17.9
	Pink sherd 2	577.1	30.2	33.5	0.377	0.376	64.6	6.5	20.8
Experimental bricks	YC 0% 750 °C	586.4	38.7	25.4	0.414	0.369	57.5	18.3	22.9
	YC 2% 750 °C	585.6	36.0	30.6	0.405	0.367	62.2	17.5	22.6
	YC 5% 750 °C	577.0	24.1	47.7	0.364	0.367	74.6	5.9	18.5
	YC 0% 900 °C	588.9	42.0	21.7	0.428	0.367	53.7	21.5	23.3
	YC 2% 900 °C	581.9	28.5	37.0	0.381	0.365	67.3	11.5	19.3
	YC 5% 900 °C	575.9	26.9	49.7	0.368	0.372	75.9	5.4	21.2
	YC 0% 1000 °C	586.3	39.2	25.6	0.415	0.369	57.6	18.5	23.3
	YC 2% 1000 °C	576.1	21.6	54.6	0.357	0.364	78.8	4.7	17.5
	YC 5% 1000 °C	573.1	26.6	48.1	0.363	0.377	74.9	2.2	21.3

addition of salt, regardless of the temperature at which they have been fired at (Fig. 3c). However, in the case of temperature measurements, (ΔE*) when comparing to YC samples fired at 750 °C, (Fig. 3d) by varying the salt content, no significant changes were noticed, except for 2% salt content between 900 °C and 1000 °C. For 0 and 5%, the colour deviation is under the value of 5 for all temperatures and therefore imperceptible to the naked eye. As such, the temperature increase appears to have little impact on the colour change.

In contrast, the colour differences are much higher when salt is added. For 5% salt content and 900 °C firing temperature, the deviation can reach 27 (Fig. 3). The YC 2% 750 °C sample shows only a weak chromatic deviation imperceptible to the naked eye (ΔE*<5). This deviation increases to 22 when salt content is increased to 5% while maintaining a 750 °C firing temperature. Given these results, it appears that the addition of salt to the clay has impacted the ceramic colour much more than the temperature at which it was fired.

As for the sherds from Hebron, it was noticed that the white sherds show a significant difference from the pink sherds, by a higher L* value and a weak red component, b* (Table 5).

3.3.2. *Cathodoluminescence*

Cathodoluminescence imaging allows for the observation of the variability in luminescence with the experimental bricks at different firing conditions and salt contents. This method highlights the mineralogical transformations.

With the bricks, cathodoluminescence imaging highlights the phase transformations that occurred during the firing process as a function of NaCl content. The calcite ($CaCO_3$) is characterized by the orange luminescence colour (Piponnier et al., 1997; Chapoulie et al. 2016, Chapoulie & Daniel 2007). It has a high presence at 750 °C, though begins to dissipate at 900 °C and is totally absent at 1000 °C (horizontal view in Fig. 4. Previous research has indicated that the calcite grains begin to be converted to fine grained aggregates at a temperature of 550 °C. At this point, they are also diffused into the clay matrix (Riccardi et al., 1999). The presence of calcite is visible on the YC 0 % 750 °C sample. While calcite is also still present in the YC 2 % 750 °C sample, it is not homogeneous. This indicates that the decarbonation has yet to be completed. With 5% salt added to the sample fired 750 °C the calcite has indeed totally disappeared. Moreover, the gehlenite ($Ca_2Al_2SiO_7$) characterized by the blue luminescence colour, is detected in the samples with the highest content of NaCl (5%). This is particularly prominent on the sample with 5% salt fired at 750 °C. In this sample, the microcrystals show a very intense blue colour of luminescence. The images acquired for the samples fired at 900 °C, also show the decomposition of the carbonates. The YC 0% 900 °C sample presents a weak luminescence with a red-brown matrix colour, while the YC 2% 900 °C sample shows some carbonate inclusions are present as well as white spots in the matrix. Finally, the samples fired at high temperature (Fig. 4 (YC 900 °C and 1000 °C)) show the transition from an orange matrix to a yellow matrix.

It should be highlighted that the blue luminescence colour can correspond to gehlenite or diopside (Götze et al., 2013). Furthermore, in concordance with the literature, (Piponnier et al., 1997) the presence of wollastonite should also be mentioned. Wollastonite ($CaSiO_3$) is characterized by a yellow-greenish luminescent colour, and is visible only in samples that have been fired at high temperature. The YC 5% 1000 °C sample, for example, reveals a matrix with this specific colour associated to wollastonite, suggesting new crystalline phases have been formed. This is confirmed through XRD analysis (see section 3.3.3).

3.3.2.1. X-ray diffraction. The mineralogical evolution that has occurred during firing (manifested by the successive appearance and disappearance of mineralogical phases), and the salt content of the raw material could be observed through the comparison of the XRD patterns but also by quantification using the Rietveld method (Table 4). The main XRD reflections in YC 0% 750 °C corresponds to quartz and calcite minerals and illite. The increase in the percentage of salt (at 750 °C) results in the disappearance of the Ca-carbonate phases. As a reaction of calcite within the clay, the gehlenite thus starts to form. Besides the clear evidence of the decomposition of calcite, the reflections of illite/muscovite show a decrease as well. With the addition of salt (2% to 5%), traces of newly formed minerals start to appear such as hematite, as well

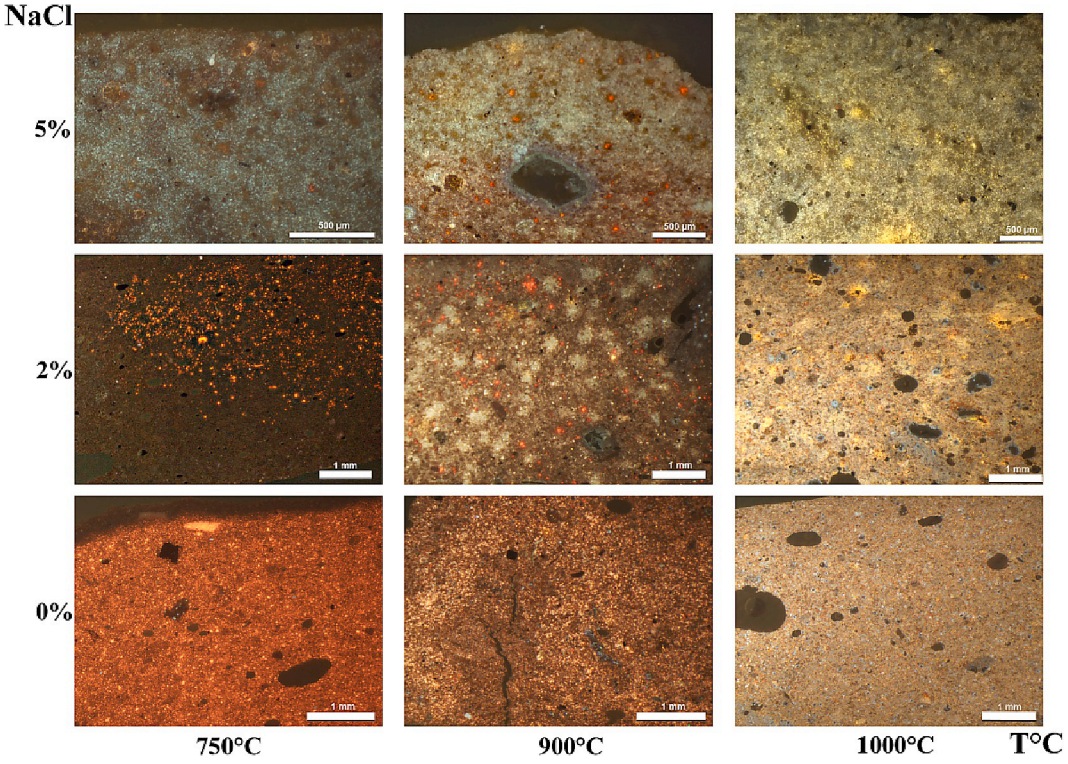

Fig. 4. Cathodoluminescence images of Ca-rich experimental bricks.

as new calcium silicates: gehlenite, pyroxene such as augite and anorthite. Gehlenite and augite start to form at temperatures between 750 °C and 900 °C. While, gehlenite formation is a result of the reaction between CaO from the carbonates and Al_2O_3 and SiO_2 from the dehydroxylated phyllosilicates (Duminuco et al., 1998; Peters and Iberg, 1978), the presence of phyllosilicates in contact with quartz and calcite allow the formation of new Ca silicates phases that can include released Mg and Na (such as augite).

The decomposition of the calcite and the newly formed phases (gehlenite and augite) demonstrated by XRD analysis strengthen the interpretation of CL-images. It also confirms the conclusion that the presence of salt accelerates and participates in the dissociation of calcite earlier in time than was previously known. Thereby, halite induces the formation of gehlenite, anorthite and augite at low temperature, increasing the reactivity between clays and Ca (Bearat et al., 1989).

Hematite formation in Ca-rich ceramics, on the other hand, is limited by the development of the new Ca-silicates, which incorporates Fe^{3+} in their network at temperatures around 900 °C to 1000 °C. This phenomenon can explain the colour saturation starting at lower temperature due to the addition of salt (De Bonis et al., 2017). These observations also indicate that the amorphous phase was involved in the melting process, producing a Fe-saturated glass, from which nano-sized hematite crystals precipitated. Low iron diffusion within the glass and short soaking time may have favored the nucleation and inhibited the crystal growth (Nodari et al., 2007). However, in this study, the hematite appears at a lower temperature (beginning at 750 °C with 2% NaCl). Gehlenite, anorthite, augite, and hematite were recorded in the pattern obtained from the Ca-rich sample, fired at 900 °C. As the quantity of salt increases, the gehlenite content begins to decrease (30% to 23%). This is in contrast with increases in augite (10% to 31%) and wollastonite (10% to 13%). Despite the addition of salt, anorthite is quite stable, but the K-Feldspars also decrease (12% to 5%) as NaCl amounts increase. Moreover, it is noted that if enough Ca is available, anorthite appears either due to the decomposition of the existing gehlenite with the amorphous matrix formed from clay minerals, dehydroxylation, or only due to the reaction of the decomposed clay minerals and CaO in the rims of the grains (Holakooei et al., 2014). According to previous studies (Piponnier et al., 1997; Traoré et al., 2000; Trindade et al., 2009), wollastonite is an intermediate compound that appears at 800 °C to 850 °C, and begins formation when the unreacted lime attacks the grains of quartz or, like with anorthite, as a result of the decomposition of gehlenite. At temperatures above 950 °C, gehlenite (considered as an intermediate compound) becomes unstable in the presence of SiO_2 and decomposes. This decomposition enables anorthite, and wollastonite to be generated (Tschegg et al., 2009). At 1000 °C, the gehlenite content decreases considerably (23% to 14%) in favor of augite again. The K-feldspars content also collapses, while wollastonite increases little, and plagioclase feldspars are stable. It is also noticeable that the mineralogical phase for anorthite begins to disappear after a temperature of 1100 °C is reached under normal conditions (Traoré et al., 2003).

The same observation was made for the gehlenite, which starts to decrease concurrent with increasing salt percentages. The hematite reflections do not present any changes, however. Their appearance starts at 750 °C within the 2% salt sample, and is similarly present at 1000 °C, with 5% salt added.

In summary, the addition of salt induces mineralogical changes including the disappearance of calcite and the appearance of Ca-silicates from 750 °C onwards. The effect of firing at higher temperatures and the salt addition facilitates the decomposition of the carbonates and silicates at lower temperatures than usual, allowing for the formation of new crystallized phases. All the Ca-rich fired samples, beginning with those with at least 2% added salt and fired at 750 °C, contained gehlenite and augite, which have been formed due to the decomposition of calcite. In addition, hematite and anorthite were formed in these samples as well. These newly formed minerals remained present throughout the entire temperature range regardless of the percentage of salt added.

3.3.2.2. SEM-EDX analyses. The SEM observations revealed the microtexture of the carbonate-rich base clay experimental bricks. It also provided information regarding the porosity and the glassy phases. The investigations of the microtexture of the sherds were made on fresh fracture surfaces and on polished thick sections. Normally the development of the crystalline and glassy phases in a ceramic is the result of the temperature of the heating treatments applied. The proportion of Fe_2O_3 is constant (~5%) in all experimental bricks, regardless of the NaCl level or the temperature applied. The bulk chemical results also reveal that the addition of the salt did not affect the chemical composition, except in the case of the potassic compound (K_2O), which decreases as salt concentration increases (Table 3). In fact, the ratio K_2O/SiO_2 decreases from 0.08 to 0.05 for samples fired at 750 °C as a result of increasing percentages of salt (Table 3). The same decrease was observed for the other temperatures, until a collapse of the rate for bricks with the highest salt content and highest firing temperature (0.02 for YC 5% 1000 °C). On the other hand, the K_2O content of the brick without salt fired at 1000 °C is slightly reduced, though still similar to the origin alone. Thus, the introduction of salt combined with an increase in the firing temperature causes the loss of this element. Picon (1991) explained the K-loss phenomenon, due to the alteration within the ceramic and highlighting the importance of different factors that contribute to the availability of silicate materials for structural rearrangements. One proposed factor is the percentages of lime in the ceramics, which can allow the development of an unstable glassy or amorphous phase, or even for the evolution of crystalline phases, which are also unstable such as gehlenite. In addition, Fabbri and Fiori (1985) presented different studies where the reaction between kaolin clays and NaCl led to the complete elimination of chlorine at about 520 °C. As for calcareous illitic-chloritic clays, the HCl was volatilized at a higher temperature and stimulated the decomposition of carbonate impurities forming potassium chloride. They observed that the addition of the NaCl caused a significant decrease in the amount of residual potassium and a progressive elimination of residual Cl in samples fired above 750 °C.

In addition, Bearat explained that the eliminated alkalis are in the form of chlorides during the firing process (1990). This means that the formation of calcium silicates promotes the formation of alkaline chlorides, which start to volatilize at temperatures of 700 °C–750 °C (Bearat, 1990). However, it is difficult to provide a complete and precise explanation of the phenomenon. The most abundant oxides are SiO_2 and Al_2O_3, which are mainly associated with the clay minerals, although often the SiO_2 content may also be associated with the quartz particles. The content of iron oxide is normally sensitive during firing. This results in variable colour and texture of the ceramic (El Ouahabi et al., 2015; El Boudour El Idrissi, 2016). In the present study, the proportion of iron in the samples does not affect the colour change.

SEM observations also revealed rhombic voids in all the experimental bricks, including those absent salts (Fig. 5). At 750 °C, rhombohedral minerals are yet present but have started to decompose. These forms are attributed to calcite or Mg-calcite minerals. With the addition of salt and/or with the increasing of firing temperature, voids are then created replacing the minerals. Furthermore, at 1000 °C the formation of a new phase can be observed inside the voids. The core presents a significant Mg enhancement, suggesting that the mineralogical phases of augite have been formed. Further observations in the clay matrix have also been recorded for the samples, including the development of the glassy phase and ellipsoidal vesicles that increase with added the salt content. The same phenomenon is known to occur with increasing temperature. The specific role of salt in promoting the development of pores in the material is currently being investigated further and will be the subject of a future publication.

4. Conclusion

The study confirmed the role of halite in the bleaching of ceramics with a high CaO content. Indeed, colorimetric measurements carried out

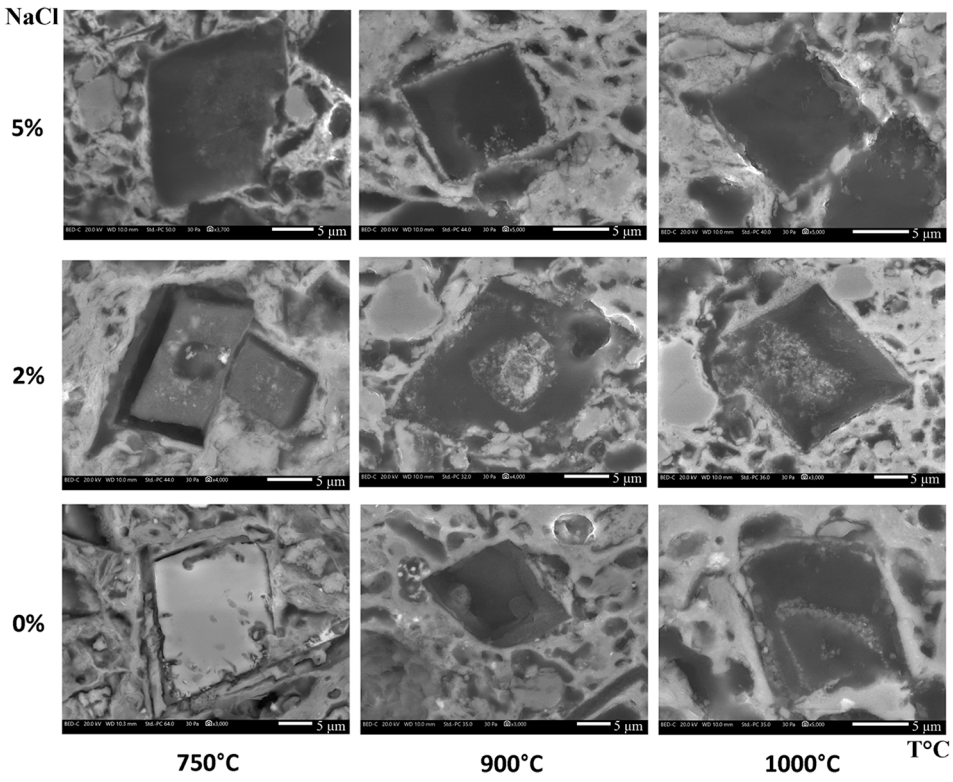

Fig. 5. SEM-BSE images of calcite or rhombohedral voids present in the matrix of the experimental bricks.

on experimental bricks with different salt contents, showed a significant loss of the red component as the salt concentration increased, as well as a loss of the yellow component to a lesser degree. These colorimetric losses are associated with a decrease of their saturation. At the same time, the clarity has significantly increased. These factors allow for the empirical characterisation of the whitening effect observed visually and confirm the main role of salt in this process, beyond the effect of temperature alone.

The mineralogical phase changes recorded in the experimental bricks manufactured in the laboratory have also been highlighted by different methods. Cathodoluminescence images showed these changes in the material. Qualitative and quantitative XRD results allowed for the documentation of the evolving proportions for these different phases, coincident with increases of salt content and firing temperature. In fact, the process of alteration of clay minerals to form new calcium silicates, appears to take place at a lower temperature in the presence of salt than has been generally thought. In this regard, significant differences in the microstructure of the calcareous clays with 5% salt are observed with the appearance of Ca-silicates (gehlenite, wollastonite) as early as 750 °C.

Furthermore, the colour changes, due to the trapping of Fe ions in the crystal lattice can now be explained (Nodari et al., 2007). Although Mossbauer measurements have not yet been carried out, Chevalier et al. (1976) have shown that gehlenite, anorthite or wollastonite crystals can trap Fe ions in their lattice, by substitution of Al^{3+} and Ca^{2+}. They pointed out that ferric oxide is known to be produced when biotite reaches high temperatures, such as 900 °C, and that crystallization improves at 1000 °C. In addition, Nöller and Knoll (1983) conducted investigations by making possible the insertion of Fe^{3+} into the lattices of Ca-Mg-Al silicates. They observed that the difference in coloration could be explained for synthetic silicates by a polarized binding of Fe^{3+} ions in a disordered matrix. Therefore, the experimental data presented here provides significant explanatory evidence for the action of NaCl on the whitening of calcareous clays. By lowering the temperature at which calcium silicates are formed, NaCl serves to reduce the necessary temperature at which the bleaching effect starts.

Moreover, the result obtained by the SEM-imagery has made it possible to more accurately describe and assign the presence of rhombohedral voids. Results show that they are due to the dissolution of the carbonates, contrary to what has been put forth previously in the scientific literature where voids had been attributed to the dissolution of salts (Rye, 1976).

Returning to the Hebron ceramics specifically, it is clear from the experimental results that the two colorations obtained (pink and white) can in fact be explained primarily by a difference in salt concentration in the initial mixture rather than other factors.

Other measurements currently underway will further consider the effect of salt on the porosity of ceramics. These observations will be compared with ceramics produced elsewhere at other sites (notably in India) where similar practices with salt addition, have been reported.

CRediT authorship contribution statement

L. Teodorescu: Conceptualization, Investigation, Writing – original draft, Writing – review & editing. **N. Cantin:** Conceptualization, Methodology, Investigation, Writing – review & editing, Validation, Visualization, Supervision, Data curation. **A. Ben Amara:** Investigation, Methodology, Writing – review & editing, Validation, Visualization, Data curation. **R. Chapoulie:** Validation, Resources, Visualization. **V. Roux:** Validation, Resources, Visualization, Supervision, Project administration.

Acknowledgements

The authors would like to thank the internal collaborators of the IRAMAT-CRP2A laboratory (especially D. Pierce for his English review and remarks, and Y. Lefrais for SEM-EDS expertise) as well as the external collaborators who contributed to this study, particularly by A. Queffelec for performing grain size analysis at PACEA Laboratory (University of Bordeaux) and A. Bocquet-Lienard CRAHAM Laboratory

(University of Caen) for providing us documentation. The sampling and study of the clay material and ceramics from Hebron is part of the project "Traditional knowledge of the Hebron's potters and Heritage Resilience (Palestinian Territories)", National Geographic Society- NGS-398R-18 (PI, V. Roux). We are thankful to the two anonymous referees for their critical reading and suggestions, which helped improving the paper.

References

Bearat, H., 1990. Etude de Quelques Altérations Physico-Chimiques des Céramiques Archéologiques. Université de Caen, France, Thèse de doctorat.

Bearat, H., Dufournier, D., Nguyen, N., Raveau, B., 1989. Influence de NaCl sur la couleur et la composition chimique des pâtes céramiques calcaires au cours de leur cuisson. Archeosciences 13, 43–53. https://doi.org/10.3406/arsci.1989.871.

Bouchet, A., Meunier, A., Sardini, P., 2000. Minéraux Argileux Structure Cristalline, Identification par Diffraction de rayons X = Clay Minerals: Crystal Structure. X-ray diffraction identification, Elf Exploration Production, Pau (Pyrénées-Atlantiques).

Brooks, D., Bieber, A.M., Harbottle, G., Sayre, E.V., 1974. Biblical studies through activation analysis of ancient pottery, in: Archaeological Chemistry, Advances in Chemistry. AMERICAN CHEMICAL SOCIETY, WASHINGTON, D. C., pp. 8–33. 10.1021/ba-1974-0138.

Chapoulie, R., Robert, B., Casenave, S., 2016. The cathodoluminescence phenomenon used for the study of ancient ceramics and stones. International Journal on Culture and Heritage at Risk – cities of memory, Edifir Florence, 1.1, 53-72.

Chapoulie, R., Daniel, F., 2007. Cathodoluminescence: recherches sur une méthode d'analyse en archéométrie. British Archaeological Reports, BAR S1700, 1-16.

Chevalier, R., Coey, J.M.D., Bouchez, R., 1976. A study of iron in fired clay : Mössbauer effect and magnetic measurements. J. Phys. Colloques 37, C6-861-C6-865. Doi: 10.1051/jphyscol:19766181.

Combès, J.-L., Louis, A., 1967. Les poteries de Djerba. Publication du centre des arts et traditions populaires, Tunis.

Cultrone, G., Rodriguez-Navarro, C., Sebastian, E., Cazalla, O., De La Torre, M.J., 2001. Carbonate and silicate phase reactions during ceramic firing. Eur. J. Mineral. 13, 621–634. https://doi.org/10.1127/0935-1221/2001/0013-0621.

De Bonis, A., Cultrone, G., Grifa, C., Langella, A., Leone, A.P., Mercurio, M., Morra, V., 2017. Different shades of red: The complexity of mineralogical and physico-chemical factors influencing the colour of ceramics. Ceram. Int. 43, 8065–8074. https://doi.org/10.1016/j.ceramint.2017.03.127.

Dufournier, D., 1982. L'utilisation de l'eau de mer dans la préparation des pâtes céramiques calcaires, premières observations sur les conséquences d'un tel traitement. Archeosciences 6, 87–100. https://doi.org/10.3406/arsci.1982.1195.

Duminuco, P., Messiga, B., Riccardi, M.P., 1998. Firing process of natural clays. Some microtextures and related phase compositions. Thermochim. Acta 321, 185–190. https://doi.org/10.1016/S0040-6031(98)00458-4.

El Boudour El Idrissi, H., Daoudi, L., El Ouahabi, M., Fagel, N., 2016. Flaws linked to lime in pottery of Marrakech (Morocco). J. Mater. Environ. Sci. 7, 3738–3745.

El Ouahabi, M., Daoudi, L., Hatert, F., Fagel, N., 2015. Modified mineral phases during clay ceramic firing. Clays Clay Miner. 63, 404–413. https://doi.org/10.1346/CCMN.2015.0630506.

Fabbri, B., Fiori, C., 1985. Influence of Sodium Chloride on Thermal Reactions of Heavy Clays During Firing, in. Clay Minerals Society, Denver.

Götze, J., Schertl, H.-P., Neuser, R.D., Kempe, U., Hanchar, J.M., 2013. Optical microscope-cathodoluminescence (OM–CL) imaging as a powerful tool to reveal internal textures of minerals. Mineral. Petrol. 107, 373–392. https://doi.org/10.1007/s00710-012-0256-0.

Holakooei, P., Tessari, U., Verde, M., Vaccaro, C., 2014. A new look at XRD patterns of archaeological ceramic bodies: An assessment for the firing temperature of 17th century haft rang tiles from Iran. JTHEA 118, 165–176. https://doi.org/10.1007/s10973-014-4012-z.

Kelly, K.L., Judd, D.B., 1976. Color : Universal Language and Dictionary of Names. National Bureau of Standards, New York, Special Publication, U.S. Dept. of Commerce, p. 440.

Konert, M., Vandenberghe, J., 1997. Comparison of laser grain size analysis with pipette and sieve analysis: a solution for the underestimation of the clay fraction. Sedimentology 44, 523–535. https://doi.org/10.1046/j.1365-3091.1997.d01-38.x.

Nodari, L., Marcuz, E., Maritan, L., Mazzoli, C., Russo, U., 2007. Hematite nucleation and growth in the firing of carbonate-rich clay for pottery production. J. Eur. Ceram. Soc. 27, 4665–4673. https://doi.org/10.1016/j.jeurceramsoc.2007.03.031.

Nöller, R., Knoll, H., 1983. Magnetic properties of calcium-silicates (diopside and gehlenite) doped with iron (III). Solid State Commun. 47, 237–239. https://doi.org/10.1016/0038-1098(83)90552-5.

Peters, T., Iberg, R., 1978. Mineralogical changes during firing of calcium-rich brick clay. Am. Ceram. Soc. Bull. 57, 503–506.

Picon, M., 1991. Quelques observations complémentaires sur les altérations de composition des céramiques au cours du temps : cas de quelques alcalins et alcalino-terreux. Archeosciences 15, 117–122. https://doi.org/10.3406/arsci.1991.1263.

Piponnier, D., Bechtel, F., Florin, D., Molera, J., Schvoerer, M., Vendrell, M., 1997. Apport de la cathodoluminescence à l'etude des transformations de phases cristallines dans des céramiques kaolinitiques carbonatées. Key Eng. Mater. 132–136, 1470–1473. https://doi.org/10.4028/www.scientific.net/KEM.132-136.1470.

Riccardi, M.P., Messiga, B., Duminuco, P., 1999. An approach to the dynamics of clay firing. Appl. Clay Sci. 15, 393–409. https://doi.org/10.1016/S0169-1317(99)00032-0.

Rye, O.S., 1976. Keeping your temper under control: materials and the manufacture of papuan pottery. Archaeol. Oceania 11, 106–137.

Traoré, K., Kabré, T.S., Blanchart, P., 2003. Gehlenite and anorthite crystallisation from kaolinite and calcite mix. Ceram. Int. 29, 377–383. https://doi.org/10.1016/S0272-8842(02)00148-7.

Traoré, K., Siméon Kabré, T., Blanchart, P., 2000. Low temperature sintering of a pottery clay from Burkina Faso. Appl. Clay Sci. 17, 279–292. https://doi.org/10.1016/S0169-1317(00)00020-X.

Trindade, M.J., Dias, M.I., Coroado, J., Rocha, F., 2009. Mineralogical transformations of calcareous rich clays with firing: a comparative study between calcite and dolomite rich clays from Algarve, Portugal. Appl. Clay Sci. 42, 345–355. https://doi.org/10.1016/j.clay.2008.02.008.

Tschegg, C., Ntaflos, T., Hein, I., 2009. Thermally triggered two-stage reaction of carbonates and clay during ceramic firing — A case study on bronze age cypriot ceramics. Appl. Clay Sci. 43, 69–78. https://doi.org/10.1016/j.clay.2008.07.029.

von der Crone, M.J., Maggetti, M., 1998. Experimental firing of clays using salt water. Presented at the Archaeometry 98, BAR International Series, Oxford, 249–255.